A tunable three layer phase mask for single laser exposure 3D photonic crystal generations: bandgap simulation and holographic fabrication

Kris Ohlinger,[1] Hualiang Zhang,[2] Yuankun Lin,[1,2,*] Di Xu,[3] and Kevin P. Chen[3]

[1]*Depatment of Physics, Univ. of North Texas, Denton, TX 76203, USA*
[2]*Department of Electrical Engineering, Univ. of North Texas, Denton, TX 76203, USA*
[3]*Dept. of Electrical and Computer Engineering, Univ. of Pittsburgh., Pittsburgh, PA 15213, USA*
**yuankun.lin@unt.edu*

Abstract: Through the use of a multi-layer phase mask to produce five-beam interference, three-dimensional photonic crystals can be formed through single exposure to a photoresist. In these holographically formed structures, the interconnectivity is controlled by the relative phase difference among contributing beams. Photonic band gaps are calculated and the simulation shows a maximum bandgap of 18% of the middle gap frequency when the phase difference is optimized. A three-layer phase mask is fabricated by placing a spacer layer between two orthogonally-orientated gratings. The phase difference is controlled by thermal-tuning of the spacer thickness. Photonic crystal templates are holographically fabricated in a photosensitive polymer using the phase mask.

©2011 Optical Society of America

OCIS codes: (160.5293) Photonic bandgap materials; (050.6875) Three-dimensional fabrication.

References and links

1. S. Noda, M. Yokoyama, M. Imada, A. Chutinan, and M. Mochizuki, “Polarization mode control of two-dimensional photonic crystal laser by unit cell structure design,” Science **293**(5532), 1123–1125 (2001).
2. T. Ergin, N. Stenger, P. Brenner, J. B. Pendry, and M. Wegener, “Three-dimensional invisibility cloak at optical wavelengths,” Science **328**(5976), 337–339 (2010).
3. K. M. Ho, C. T. Chan, C. M. Soukoulis, R. Biswas, and M. Sigalas, “Photonic band gaps in three dimensions: new layer-by-layer periodic structures,” Solid State Commun. **89**(5), 413–416 (1994).
4. A. Blanco, E. Chomski, S. Grabtchak, M. Ibisate, S. John, S. W. Leonard, C. Lopez, F. Meseguer, H. Miguez, J. P. Mondia, G. A. Ozin, O. Toader, A. Geoffrey, O. Toader, and H. M. van Driel, “Large-scale synthesis of a silicon photonic crystal with a complete three-dimensional bandgap near 1.5 micrometres,” Nature **405**(6785), 437–440 (2000).
5. M. Deubel, G. von Freymann, M. Wegener, S. Pereira, K. Busch, and C. M. Soukoulis, “Direct laser writing of three-dimensional photonic-crystal templates for telecommunications,” Nat. Mater. **3**(7), 444–447 (2004).
6. M. Campbell, D. N. Sharp, M. T. Harrison, R. G. Denning, and A. J. Turberfield, “Fabrication of photonic crystals for the visible spectrum by holographic lithography,” Nature **404**(6773), 53–56 (2000).
7. S. Yang, M. Megens, J. Aizenberg, P. Wiltzius, P. M. Chaikin, and W. B. Russel, “Creating periodic three-dimensional structures by multibeam interference of visible laser,” Chem. Mater. **14**(7), 2831–2833 (2002).
8. T. Y. M. Chan, O. Toader, and S. John, “Photonic band-gap formation by optical-phase-mask lithography,” Phys. Rev. E Stat. Nonlin. Soft Matter Phys. **73**(4), 046610 (2006).
9. O. Toader, T. Y. M. Chan, and S. John, “Diamond photonic band gap synthesis by umbrella holographic lithography,” Appl. Phys. Lett. **89**(10), 101117 (2006).
10. Y. Zhong, L. Wu, H. Su, K. S. Wong, and H. Wang, “Fabrication of photonic crystals with tunable surface orientation by holographic lithography,” Opt. Express **14**(15), 6837–6843 (2006), http://www.opticsinfobase.org/oe/abstract.cfm?URI=oe-14-15-6837.
11. Y. K. Pang, J. C. Lee, C. T. Ho, and W. Y. Tam, “Realization of woodpile structure using optical interference holography,” Opt. Express **14**(20), 9113–9119 (2006), http://www.opticsinfobase.org/oe/abstract.cfm?URI=oe-14-20-9113.
12. Y. Lin, P. R. Herman, and K. Darmawikarta, “Design and holographic fabrication of tetragonal and cubic photonic crystals with phase mask: toward the mass-production of three-dimensional photonic crystals,” Appl. Phys. Lett. **86**(7), 071117 (2005).
13. Y. Lin, A. Harb, D. Rodriguez, K. Lozano, D. Xu, and K. P. Chen, “Fabrication of two-layer integrated phase mask for single-beam and single-exposure fabrication of three-dimensional photonic crystal,” Opt. Express **16**(12), 9165–9172 (2008), http://www.opticsexpress.org/abstract.cfm?URI=OPEX-16-12-9165.

#148825 - $15.00 USD Received 7 Jun 2011; revised 17 Aug 2011; accepted 21 Aug 2011; published 24 Aug 2011

14. D. Chanda, L. E. Abolghasemi, M. Haque, M. L. Ng, and P. R. Herman, "Multi-level diffractive optics for single laser exposure fabrication of telecom-band diamond-like 3-dimensional photonic crystals," Opt. Express **16**(20), 15402–15414 (2008), http://www.opticsexpress.org/abstract.cfm?URI=OPEX-16-20-15402.
15. D. Xu, K. P. Chen, A. Harb, D. Rodriguez, K. Lozano, and Y. Lin, "Phase tunable holographic fabrication for three-dimensional photonic crystal templates by using a single optical element," Appl. Phys. Lett. **94**(23), 231116 (2009).
16. G. Y. Dong, L. Z. Cai, X. L. Yang, X. X. Shen, X. F. Meng, X. F. Xu, and Y. R. Wang, "Holographic design and band gap evolution of photonic crystals formed with five-beam symmetric umbrella configuration," Opt. Express **14**(18), 8096–8102 (2006), http://www.opticsexpress.org/abstract.cfm?URI=OPEX-14-18-8096.
17. S. G. Johnson and J. D. Joannopoulos, "Block-iterative frequency-domain methods for Maxwell's equations in a planewave basis," Opt. Express **8**(3), 173–190 (2001), http://www.opticsexpress.org/abstract.cfm?URI=OPEX-8-3-173.
18. Y. Lin, D. Rivera, and K. P. Chen, "Woodpile-type photonic crystals with orthorhombic or tetragonal symmetry formed through phase mask techniques," Opt. Express **14**(2), 887–892 (2006), http://www.opticsinfobase.org/oe/abstract.cfm?URI=oe-14-2-887.

1. Introduction

Photonic bandgap materials (also called photonic crystals (PhCs)) are periodic dielectric nano/micro-structures. PhCs have attracted substantial interest due to their varied potential applications [1]. Very recently, a combination of three-dimensional (3D) PhCs with transformation optics has generated cloaking devices [2]. One-dimensional and two-dimensional PhCs can be fabricated easily for applications such as Bragg gratings and integrated laser on chip [1]. However nano/micro-fabrication of three-dimensional (3D) photonic crystals with large photonic bandgaps, especially at a large-scale, has been a challenge over the past decade. Several techniques have succeeded in fabricating 3D PhCs, such as e-beam lithography for multilayer stacking of woodpile-like structures [3], colloidal self-assembly [4,5], multi-photon direct laser writing [2,6], and holographic lithography [7,8]. With holographic lithography, 3D interference patterns are generated with multiple coherent laser beams and 3D structure templates are formed by recording the interference pattern in a photoresist. The structure and symmetry of the interference pattern can be controlled by the beam propagating direction, the number of the interfering beams, the beam intensities, their respective polarizations and their relative phases [9,10]. So far holographic lithography has been successful in fabricating large-volume PhC templates at sub-micro/nano-scales [7–15].

However, the optical alignment for multiple-beam holographic lithography is very complicated if using mirrors, polarizers and beam splitters. In order to simplify the optical setup and improve the optical stability, a single optical element such as a refractive or diffractive optical element has recently been used for laser holographic fabrication of 3D PhC structures [11–15]. A flat-top prism and multi-layer phase mask [13–15] have been demonstrated to fabricate diamond-like PhC templates by introducing a phase difference among the diffracted beams. Overall the single-beam and single-exposure process using a single optical element for holographic lithography has drastically reduced the fabrication complexity.

Several groups have calculated photonic bandgap structures for photonic crystals produced using five-beam inference [8,9,16]. The maximum photonic bandgaps were found to be as high as 25% with careful selection of beam polarizations and their intensities. In reality, the polarization of interfering beams and their respective beam intensities are determined by the diffraction direction and diffraction efficiency of a phase mask. These parameters are not as arbitrary as those used in other group's calculation. In this paper, we calculate the photonic band gap in holographically-formed 3D photonic structures through the phase mask technique. The photonic band gaps are varied with the phase difference among the interfering beams and also with dielectric material filling factors in the 3D microstructure. We also fabricate a multi-layer phase mask and control the phase delay for two interfering beams. 3D photonic crystal templates are fabricated with the phase mask.

#148825 - $15.00 USD Received 7 Jun 2011; revised 17 Aug 2011; accepted 21 Aug 2011; published 24 Aug 2011
(C) 2011 OSA

2. Holographic photonic structures formed through phase mask based interference and photonic band gap simulation

Five-beam interference can be used to form 3D interconnected nano/micro-structures if there is a phase delay for one or two interfering beams [9,13–15]. A scheme of the multi-layer phase mask is shown in Fig. 1. The multi-layer phase mask consists of a spacer layer between two orthogonally-orientated gratings. When a single circularly-polarized beam goes through such a phase mask, there are five low-order diffracted beams behind the phase mask, namely the (0, 0), (0, ± 1) and (± 1, 0) beams as shown in Fig. 1(a), and second-order diffracted beams (1,1), (1,-1), (−1,1), and (−1, −1). Usually, second-order beams are weak and can be neglected.

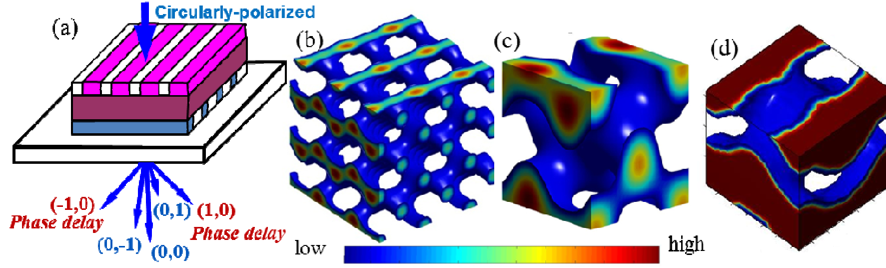

Fig. 1. (a) A scheme of three-layer phase mask; (b) Iso-intensity surface of five-beam interference pattern with phase shift of 0.5 π; (c) enlarged view of the five-beam interference pattern; (d) Binary dielectric structure output from the MIT Photonic-bands Package.

The five 0th and 1st order diffracted beams can be described by Eqs. (1)–(5):

$$\mathbf{E}_{0,0}(\mathbf{r},t)=\mathbf{E}_{0,0}\cos((k_{0,0}\bullet r-\omega t+\delta_2), \quad (1)$$

$$\mathbf{E}_{1,0}(\mathbf{r},t)=\mathbf{E}_{1,0}\cos((k_{1,0}\bullet r-\omega t+\delta_1), \quad (2)$$

$$\mathbf{E}_{-1,0}(\mathbf{r},t)=\mathbf{E}_{-1,0}\cos((k_{-1,0}\bullet r-\omega t+\delta_1), \quad (3)$$

$$\mathbf{E}_{0,1}(\mathbf{r},t)=\mathbf{E}_{0,1}\cos((k_{0,1}\bullet r-\omega t+\delta_2), \quad (4)$$

$$\mathbf{E}_{0,-1}(\mathbf{r},t)=\mathbf{E}_{0,-1}\cos((k_{0,-1}\bullet r-\omega t+\delta_2), \quad (5)$$

where k and ω are the wave vector and angular frequency of the beam, respectively, $\boldsymbol{E}$ is the constant of electric field strength, and δ is the initial phase of the beam. When a single beam goes through the top grating, the diffracted beams (1,0) and (−1,0) have a longer optical path than the (0,0) beam. Initial phases for beams (0, 0), (0, 1) and (0, −1) are the same, but different from those for beams (1, 0), and (−1, 0), i.e. the δ_1 and δ_2 are different in the above equations.

The intensity of the 1st order beam is low due to the low diffraction efficiency of the phase mask. For a fabricated phase mask in this paper, the ratio of beam intensity for 0th, 1st and 2nd order diffracted beams versus incident beam is 50%,10%, 1.5%, respectively, with 4% of incident beam is reflected. Other experimental measurements [14] have reported diffraction efficiencies of 48% for (0, 0), 15% for (0, 1) and (0, −1), and 8% for (1, 0) and (−1, 0). In our simulation, we set the ratio of electrical field strength $E_{00}:E_{10}:E_{-10}:E_{0-1}:E_{01}$ = 2.236:1:1:1:1, which is same as experimental values. The interfering angle between 0th order and 1st order beam is set to be 70° degree (If it is 70.53° degree, the produced structure has face-centered-cubic symmetry). Figure 1(b) shows the simulated five-beam interference pattern with δ_2-δ_1 = 0.5π using the following equation:

#148825 - $15.00 USD Received 7 Jun 2011; revised 17 Aug 2011; accepted 21 Aug 2011; published 24 Aug 2011
(C) 2011 OSA

$$I(r) = I_0 + \Delta I(r) = <\sum_{i=1}^{5} E_i^2(r,t)> + 2\sum_{i<j}^{5} E_i \cdot E_j \cos[(k_i - k_j) \cdot r + (\delta_i - \delta_j)]$$

The enlarged view of the interference pattern is shown in Fig. 1(c). The iso-intensity surface is illustrated by different colors. For the photonic band structure simulation, the interference pattern is conversed to silicon structure (dielectric constant = 11.9) using the following step functions:

$\varepsilon(r) = 1$ when $I < I_{th}$

$\varepsilon(r) = 11.9$ when $I > I_{th}$

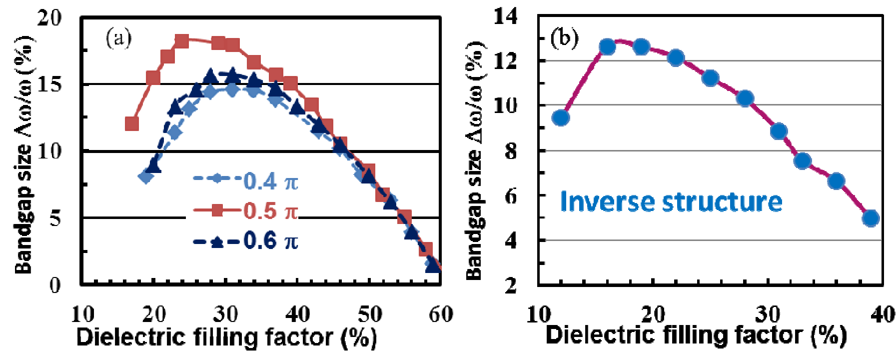

Fig. 2. Photonic band gap size as a function of dielectric filling factors (a) for phase delay δ_2-δ_1 = $0.4\ \pi$, $0.5\ \pi$, and $0.6\ \pi$ in holographic structures where the high intensity volume is replaced by a material with dielectric constant of 11.9; (b) for phase delay δ_2-δ_1 = $0.5\ \pi$ in an inverse structure where the low intensity holographic volume is replaced by a material with dielectric constant of 11.9.

Band gap calculations, using MIT Photonic-Bands (MPB) package [17], were performed for the formed structures through the above binarization. To check for correct interpretation of the structure, an output of a dielectric structure was generated and shown in Fig. 1(d) with a different length scales and dielectric filling factor. The interface shows the averaging that is done to the step index interface by MPB. The dielectric filling factor was calculated during the conversion of the interference volume into a binary dielectric material system. Photonic band gaps were calculated as a function of the dielectric filling factors for binary dielectric structure formed with an interfering angle of 70 degrees between 0th and 1st order beams. Figure 2(a) shows the photonic band gap for holographic structures where the high-intensity volume is replaced by silicon and the low-intensity volume is replaced by air. Photonic band gaps appear at filling factors between 0.1 and 0.6, similar to other group's simulation results [16]. A maximum band gap of 18% of the middle gap frequency is found for dielectric filling factors in ranges of 24-31%. This is in contrast to a maximum band gap of 25% that has been reported in ideal photonic structures which were generated by optimizing individual beam polarizations for maximum band gaps [8,9,16]. However the single and circularly polarized beam based phase mask method has significantly simplified the optical setup and fabrication process.

Figure 2(a) also shows photonic band gap sizes for different phase delays δ_2-δ_1 = $0.4\ \pi$, $0.5\ \pi$, and $0.6\ \pi$. These three curves have a similar trend of band gap size change relative to the filling factor, i.e. the band gap size shows maximum around the filling factor of 28%. The relatively higher photonic band gaps associated with a phase shift of 0.5 π is in agreement with the generation of a high symmetric structure [9]. With phase shifts of $0.4\ \pi$, and $0.6\ \pi$, the band gap size can reach as high as 15%. The results indicate that the multi-layer phase mask based singe beam and singe exposure process is a robust method for the fabrication of photonic crystals with large photonic band gaps.

#148825 - $15.00 USD Received 7 Jun 2011; revised 17 Aug 2011; accepted 21 Aug 2011; published 24 Aug 2011
(C) 2011 OSA

Figure 2(b) shows photonic band gap size as a function of dielectric filling factors in inverse holographic structures with the low intensity volume replaced by a material with dielectric constant of 11.9 and with a phase delay δ_2-δ_1 = $0.5\ \pi$. A maximum band gap size of 12% is found in the inverse structure around dielectric filling factor of 18%.

3. Fabrication of three-layer phase mask and holographic photonic crystal template

In order to prove the concept, a three-layer phase mask was fabricated with two orthogonally orientated gratings separated by a spacer. The fabrication of a three-layer phase mask was divided into two procedures: the fabrication of a grating mold in Polydimethylsiloxane (PDMS) and the imprinting of two gratings in SU8. The mother mold of the grating was fabricated in dipentaerythritol penta/hexaacrylate (DPHPA) photoresist using a two-beam interference method [13]. A subsequent pattern inversion transfers the mother grating into a daughter PDMS grating mold. The PDMS grating mold was then used to imprint grating patterns on pure SU8-2035 photoresist (MicroChem Inc.) coated on a glass slide under a flood UV irradiation source (UL500P, Hoya-Schott Co.) for 1 min. The exposed SU8 was partially polymerized by post-baking at 65°C for 10min. The PDMS mold is then peeled away from the SU8.

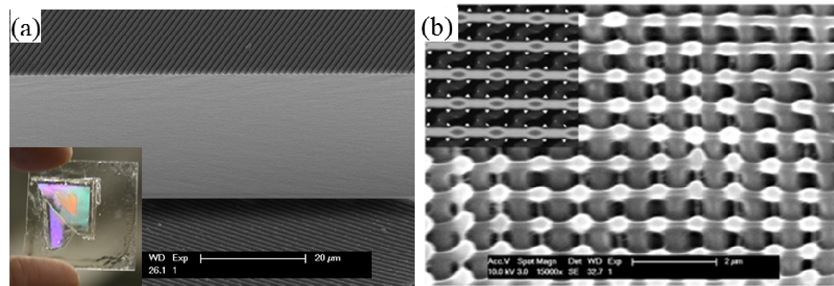

Fig. 3. (a) SEM image of three-layer phase mask with two orthogonal gratings separated by a spacer. The inset shows a photograph of the mask. (b) Fabricated photonic crystal templates in DPHPA using the phase mask. The inset is the simulated structure for a comparison.

To produce the second grating and spacer layer, a SU8 thin film was coated directly on the PDMS mold by a spin-coating process. The spin speed determines the film thickness which is related to the spacer thickness between gratings. After an UV exposure to the SU8 film coated on the PDMS mold, both SU8 layers are brought into contact to form a three-layer structure with two grating grooves perpendicular to each other, using a Newport precision rotation stage. An angular error from the rotation stage can result in an orthorhombic crystal structure with a viable photonic bandgap [18]. The three-layer structure was bonded at 95°C for 20 min under 50 kPa pressure. The three-layer phase mask was further hardened by a hard-baking process at 200°C for another 20 minutes. The spacer layer between two gratings is about 22 μm thick, which is produced by the spin-coating process at 2000 rpm. The spacer thickness is large enough for an efficient thermal expansion which is required for a phase tuning. A scanning electron microscope (SEM) image of a bound three-layer phase mask is shown in Fig. 3(a). Two gratings with orthogonal orientations are clearly visible on top and bottom of a spacer layer. The grating is uniform over an area of 0.5x1 cm^2. An inset in Fig. 3(a) shows a photograph of the fabricated three-layer phase mask. The phase mask has a size 0.5x0.5 cm^2. The color changes from areas of 1D grating to three-layer section. Central phase mask section (orange color) is uniform over area of 0.3x0.3 cm^2.

This three-layer phase mask was then used to produce 3D PhC templates in DPHPA photoresist through a single laser exposure process [13]. For δ_2-δ_1 being odd integral multiples of π/2, the 3D holographic interference pattern will be an interconnected woodpile structure as shown in the 3D simulation in the inlet of Fig. 3(b). The phase delay δ_2-δ_1 of π/2 is corresponding to a thickness change of $(\lambda/4n)/[(1/\cos\theta)-1]$, i.e. 498 nm, given the period of the phase mask. To yield interconnected 3D structures, a thermal tuning of spacer thickness was

#148825 - $15.00 USD Received 7 Jun 2011; revised 17 Aug 2011; accepted 21 Aug 2011; published 24 Aug 2011
(C) 2011 OSA

used to adjust the phase delay induced by the as-fabricated three-layer phase mask. The thermal expansion coefficients of the hard baked SU8 samples (n = 1.67 at 514.5nm) were reported as 102 ppm/°C for in-plane and 253 ppm/ °C for out-of plane (thickness direction) . Thus, for a 22 µm thick intermediate layer, the phase delay δ_2-δ_1 can be tuned at a rate of 0.011rad/ °C by changing the temperature.

The phase mask was mounted on a metal frame holder on a hot plate. The ambient temperature of the phase mask was raised by 30 degrees each step from 20 °C to 240 °C. The phase change was estimated to be π/8 for every 30°C temperature increment by comparing the simulation with the SEM image of samples, which is close to π/9 estimated from the thermal expansion coefficient. More accurate phase control can be realized with a spatial light modulator using electrical tuning. Once the temperature of the phase mask is stabilized, the photoresist film of DPHPA was placed in close proximity to the phase mask for laser exposure. The laser exposure time was typically between 1 and 2 s depending on the laser power and the samples were taken off rapidly after exposure. Figure 3(b) shows SEM image of the 3D PhC template in DPHPA by using the thermally controlled three-layer phase mask. The surface morphology closely matches the simulated structure in the inlet with a phase delay $\Delta\delta = \delta_2 - \delta_1 = \pi/2$. These results clearly demonstrated the fabrication of 3D photonic crystal templates through the single beam, single mask and single laser exposure process.

4. Conclusion

The photonic band structure simulation reveals band gap sizes as high as 18% in holographic dielectric structures formed through three-layer phase mask based on the single beam, single mask, and single laser exposure process. The three-layer phase mask based holographic lithography not only simplifies the optical setup, but also produces useful photonic structures with large band gaps. A three-layer phase mask is fabricated and used for the fabrication of 3D photonic crystal templates.

Acknowledgment

This work is supported by research grants from the U.S. National Science Foundation under Grant Nos. CMMI-0900564, DMR-0934157, CMMI 1115903, and CMMI-1109971.

#148825 - $15.00 USD Received 7 Jun 2011; revised 17 Aug 2011; accepted 21 Aug 2011; published 24 Aug 2011
(C) 2011 OSA